Nonperturbative QCD corrections to electroweak observables

Dru B. Renner[*]
Thomas Jefferson National Accelerator Facility (JLab)
E-mail: dru@jlab.org

Xu Feng

High Energy Accelerator Research Organization (KEK)

Karl Jansen

Deutsches Elektronen-Synchrotron (DESY)

Marcus Petschlies

The Cyprus Institute

Nonperturbative QCD corrections are important to many low-energy electroweak observables, for example the muon magnetic moment. However, hadronic corrections also play a significant role at much higher energies due to their impact on the running of standard model parameters, such as the electromagnetic coupling. Currently, these hadronic contributions are accounted for by a combination of experimental measurements, effective field theory techniques and phenomenological modeling but ideally should be calculated from first principles. Recent developments indicate that many of the most important hadronic corrections may be feasibly calculated using lattice QCD methods. To illustrate this, we will examine the lattice computation of the leading-order QCD corrections to the muon magnetic moment, paying particular attention to a recently developed method but also reviewing the results from other calculations. We will then continue with several examples that demonstrate the potential impact of the new approach: the leading-order corrections to the electron and tau magnetic moments, the running of the electromagnetic coupling, and a class of the next-to-leading-order corrections for the muon magnetic moment. Along the way, we will mention applications to the Adler function, which can be used to determine the strong coupling constant, and QCD corrections to muonic-hydrogen.

[*]Speaker.

1. Introduction

Many precision experiments are increasingly becoming sensitive to nonperturbative QCD corrections. For example, the measurement of the magnetic moment of the muon currently shows a discrepancy with the standard model of over three standard deviations. Its theoretical uncertainty is dominated by hadronic effects, making the muon g-2 a prominent example of the importance of a fully nonperturbative determination of hadronic corrections. This is just one example. The significance of QCD corrections to otherwise precision observables will increase with the experimental programs envisioned for the future. In many cases, the discovery of physics beyond the standard model may depend on accurate control of these hadronic effects.

In these proceedings, we will discuss several opportunities for lattice QCD calculations of hadronic corrections to important measurements that may in fact be more feasible than previously thought. The QCD corrections to the muon g-2 will serve as a concrete example. This will allow us to identify an issue that makes the calculation of these quantities more difficult and then describe a modified method that was introduced to alleviate this problem [1]. Additionally, there is a growing lattice effort on precisely this quantity and we will review the latest results.

After having laid the groundwork with the muon g-2, we will continue with several additional examples that illustrate the potential impact of the modified technique. We will examine the leading-order hadronic corrections for the electron and tau magnetic moments and the leading QCD contributions to the running of the QED coupling. Additionally, we will note applications to the Adler function, the determination of the strong coupling constant and the QCD corrections to the energy levels of muonic-hydrogen. We will then close with a calculation of the next-to-leading-order vacuum-polarization corrections to the muon g-2.

2. Leading-order QCD correction to the muon magnetic moment

The BNL measurement of the anomalous magnetic moment of the muon $a_\mu = (g_\mu - 2)/2$ [2] and the standard model estimate thereof [3] differ by more than three standard deviations. This discrepancy may indicate physics beyond the standard model, but making such a statement definitively requires a thorough understanding of all sources of uncertainty and ideally a significantly larger discrepancy. The experimental community is pursuing two future muon g-2 experiments at Fermilab [4] and J-PARC [5], aiming to improve the experimental precision on a_μ from $6.3 \cdot 10^{-10}$ to $(1-2) \cdot 10^{-10}$. Since $a_\mu \approx 1.2 \cdot 10^{-3}$, the new experiments will reduce the relative precision from $0.5 \cdot 10^{-6}$ to $0.9 \cdot 10^{-7}$. At this precision, the comparison between theory and experiment would be dominated by the standard model uncertainties alone, hence improvement from the theory side is highly desirable.

The value of a_μ receives contributions from all parts of the standard model, each contributing to the theoretical uncertainty as shown in table 1. Quite clearly, the standard model uncertainty is overwhelmingly dominated by hadronic physics. The total QCD contribution a_μ^{QCD} can be organized as an expansion in the QED coupling α as follows

$$a_\mu^{\text{QCD}} = \alpha^2 A_\mu^{(2)} + \alpha^3 A_\mu^{(3)} + \mathcal{O}(\alpha^4) = a_\mu^{(2)} + a_\mu^{(3)} + \mathcal{O}(\alpha^4), \qquad (2.1)$$

Contribution	Error $[10^{-10}]$
QCD-LO	5.3
QCD-NLO	3.9
QED/EW	0.2
Total	6.6

Table 1: Standard model uncertainties in a_μ [3]. The contributions QCD-LO and QCD-NLO refer to $a_\mu^{(2)}$ and $a_\mu^{(3)}$ in equation 2.1. All remaining contributions are collected together and labeled QED/EW.
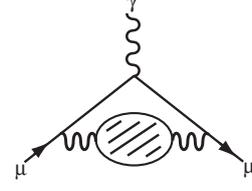
Figure 1: Leading-order QCD contribution $a_\mu^{(2)}$. The QCD contribution to $a_\mu^{(2)}$, denoted by the shaded region, can be related to $R(s)$, given in equation 2.2, determined experimentally or calculated using lattice QCD.

where $a_\mu^{(n)} = \alpha^n A_\mu^{(n)}$. The expansion in α is perturbative but the $A_\mu^{(n)}$ must be calculated nonperturbatively. The largest source of uncertainty is due to $a_\mu^{(2)}$, which we discuss next.

2.1 Experimental determination of $a_\mu^{(2)}$

The leading-order correction $a_\mu^{(2)}$, shown in figure 1, can be determined experimentally. It can be written as an integral of $R(s)$ and a known function $K(s/m_\mu^2)$ as [3]

$$a_\mu^{(2)} = \alpha^2 \int_{4m_\pi^2}^{\infty} \frac{ds}{s} K(s/m_\mu^2) R(s) \quad \text{with} \quad R(s) = \frac{\sigma(\gamma^* \to \text{hadrons})}{\sigma(\gamma^* \to e^+ e^-)}. \tag{2.2}$$

In practice, measurements of $\sigma(\gamma^* \to \text{hadrons})$ from many different experiments are combined to form the integral above. The most recent compilation of measurements results in $a_\mu^{(2)} = 6.923\,(42) \cdot 10^{-8}$ [6], which is an improvement on the error given in table 1. This approach has been and will continue to be for some time the most accurate means of providing the QCD input needed to form the standard model prediction for a_μ. This value is significantly more precise than current lattice results, but we should bear in mind that this result requires a substantial experimental effort to determine a quantity that should in principle be predicted from the theory itself. Reaching and even exceeding the precision of the experimental determination of $a_\mu^{(2)}$ should be part of the long-term efforts of the lattice community.

2.1.1 Estimates of the flavor dependence of $a_\mu^{(2)}$

As we will see shortly, lattice calculations must include the four lightest quarks to reach the precision on $a_\mu^{(2)}$ needed for the future muon g-2 experiments. However, the number of quark flavors used in current lattice computations varies from $n_f = 2$ to 3 and just recently 4 flavors. Thus it is useful to have some guidance on the n_f dependence of $a_\mu^{(2)}$. Unfortunately, there is no unique way to do this for $a_\mu^{(2)}$, which is a problem for many other observables as well. The effects of decoupling a quark flavor depend on the renormalization conditions used for the remaining degrees of freedom. This ambiguity exists in perturbation theory and would also apply to any analysis of the experimental results. The advantage of lattice calculations is that they can provide a well-defined way to prescribe such a definition.
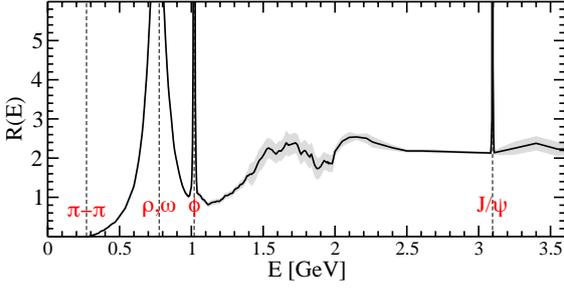
Figure 2: Measured $R(E)$. The $R(s)$ with $\sqrt{s} = E$ from F. Jegerlehner [7] is shown.

n_f	$a^{(2)}_{\mu,n_f}$ [Exp]	$a^{(2)}_{\mu,n_f}$ [Lat]
5	6.93 (06)	-
4	6.93 (06)	underway [8]
3	6.81 (05)	6.41 (46) [9], 6.18 (64) [10]
2	5.67 (05)	5.72 (16) [1], 5.46 (66) [10]

Table 2: Estimated n_f dependence of $a^{(2)}_\mu$ (given in units of 10^{-8}) from experimental measurements using equation 2.3 ("[Exp]") and current lattice calculations ("[Lat]").

Keeping in mind these limitations, we proceed with a simple means of estimating the flavor contributions from the experimental measurements. We start with the experimentally determined $R(s)$ [7] and rescale by the electric charges Q_f of the relevant quark flavors f as follows

$$ R_{n_f}(s) \equiv R(s) \frac{\sum_f^{n_f} Q_f^2}{\sum_f^n Q_f^2} \quad \text{for} \quad 4m_n^2 \le s \le 4m_{n+1}^2 \quad \text{with} \quad a^{(2)}_{\mu,n_f} \equiv \alpha^2 \int_{4m_\pi^2}^\infty \frac{ds}{s} K(s/m_\mu^2) R_{n_f}(s). \quad (2.3) $$

The $\sum_f^n$ accounts for the n degrees of freedom present in the experimental measurements between the quark thresholds $4m_n^2$ and $4m_{n+1}^2$ and the $\sum_f^{n_f}$ restores the desired n_f flavors. The leading-order perturbative contribution to $R(s)$ scales this way, so this prescription is valid up to perturbative corrections and away from the resonance regions. Near resonances, this amounts to a quark-hadron duality argument. For example, the strange quark content of the prominent ϕ meson would not follow such a scaling but the integrand $K(s/m_\mu^2)$ is relatively smooth and effectively averages $R(s)$ across a window in s over which this scaling is expected to be more effective. In practice, the part of this prescription that has the most impact on the resulting estimates of $a^{(2)}_{\mu,n_f}$ is the use of quark masses rather than a resonance mass to define the thresholds. And in fact, only the strange quark threshold is particularly sensitive to this choice.

Using this simple prescription, the n_f dependence of $a^{(2)}_\mu$ can be estimated. To do this, we have used the $R(s)$ compiled by F. Jegerlehner [7]. This is shown in figure 2. The results of this procedure and a comparison with the current lattice calculations are given in table 2. This suggests that the charm quark correction is roughly $1.2 \cdot 10^{-9}$. The current experimental precision is $6.3 \cdot 10^{-10}$, which makes it clear that charm quark contributions are already necessary to reach the precision of the BNL measurement, let alone the precision for the future g-2 experiments.

Alternatively, one could attempt to assign flavor weights to each of the final states in the total cross section $\sigma(\gamma^* \to \text{hadrons})$ and form $a^{(2)}_{\mu,n_f}$. This approach is an alternative prescription to the one given above and, in fact, differs from it [11, 12], illustrating the ambiguity in extracting the $n_f = 2$ piece. It turns out to lead to a larger $n_f = 2$ contribution than given in recent $n_f = 2$ lattice calculations, but we want to emphasize that any such ambiguities are systematically eliminated as the lattice calculations account for all the relevant quark flavors, which appears to be $n_f = 4$.

2.2 Lattice calculation of $a^{(2)}_\mu$

The standard method to calculate $a^{(2)}_\mu$ using lattice QCD was given by Blum in [13]. It requires
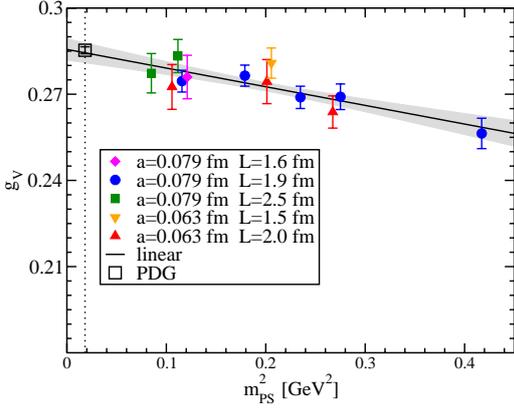
Figure 3: Vector-meson coupling g_V.
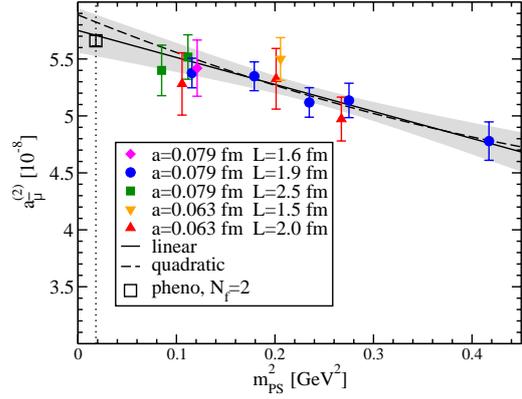
Figure 4: Modified method $a_{\overline{\mu}}^{(2)}$.

calculating the vacuum-polarization function $\Pi(Q^2)$ and evaluating the integral

$$a_\mu^{(2)} = \alpha^2 \int_0^\infty \frac{dQ^2}{Q^2} \omega(Q^2/m_\mu^2)\Pi_R(Q^2). \tag{2.4}$$

The weight function ω accounts for the perturbative portion of the diagram in figure 1 and is known. $\Pi_R(Q^2)$ is the once-subtracted vacuum-polarization function, $\Pi_R(Q^2) \equiv \Pi(Q^2) - \Pi(0)$, where Π is given by

$$(Q_\mu Q_\nu - Q^2\delta_{\mu\nu})\Pi(Q^2) \equiv \int d^4X e^{iQ\cdot(X-Y)}\langle J_\mu(X)J_\nu(Y)\rangle,$$

and is directly calculable in Euclidean space. This formulation can be related to the approach used to experimentally determine $a_\mu^{(2)}$ by noting that $R(s)$ is proportional to $\mathrm{Im}\Pi(-s+i\varepsilon)$, which is non-zero only on the branch cut starting at $s = 4m_\pi^2$. A standard dispersion analysis then allows one to relate equations 2.2 and 2.4.

2.2.1 Role of external leptonic scale in $a_\mu^{(2)}$

Naively, the lattice calculation of $a_\mu^{(2)}$ should be relatively easy. The only non-trivial part of the computation is the calculation of the Euclidean two-point correlation function $\langle J_\mu(X)J_\nu(Y)\rangle$, which can be accurately determined. Furthermore, the quantity $a_\mu^{(2)}$ is dimensionless, so it seems reasonable to expect that it may exhibit a relatively mild dependence on the scales in the problem, particularly the quark masses and lattice spacing. (Figure 3 shows an example of a typical dimensionless quantity.) However, $a_\mu^{(2)}$ is dimensionless only at the expense of introducing an external scale, the muon mass m_μ, and this has several consequences.

First, m_μ introduces a dependence on the lattice spacing a in an otherwise dimensionless observable. We can see this by writing the integration variable for $a_\mu^{(2)}$ in lattice units

$$a_\mu^{(2)} = \alpha^2 \int_0^\infty \frac{d\hat{Q}^2}{\hat{Q}^2} \omega(\hat{Q}^2/(am_\mu)^2)\Pi_{\mathrm{lat}}(\hat{Q}^2)$$

where $\hat{Q} \equiv aQ$ is the momentum variable in lattice units and $\Pi_{\mathrm{lat}}(\hat{Q}^2) \equiv \Pi_R(\hat{Q}^2/a^2)$ is directly calculated in lattice units. Thus the lattice spacing a is needed in physical units to form am_μ. This

suggests that $a_\mu^{(2)}$ may behave more like a dimensionful quantity. As a second consequence, the introduction of m_μ also allows for a stronger quark mass dependence than might otherwise be expected. The dominant contribution of the lightest vector-meson with mass m_V and electromagnetic coupling g_V is proportional to $g_V^2 m_\mu^2/m_V^2$. This is a model-dependent statement, but it is suggestive that $a_\mu^{(2)}$ may in fact behave more like a mass dimension -2 observable. (A plot of m_V corresponding to the g_V in figure 3 is given in [1].)

These two observations can be made precise by introducing an effective dimension

$$d_{\text{eff}}[X] \equiv -\frac{a}{X} \left.\frac{\partial X}{\partial a}\right|_g .$$

This quantity is defined so that it is sensitive to only QCD scales rather than the overall dimension. To accomplish this, we write the observable X as a function of both the lattice spacing a and the coupling g separately $X = X(a, g)$. Of course, $a = a(g)$ is eventually chosen to be some function of the coupling, but treating a and g separately allows us to isolate the impact of the scale setting on the quantity X. Furthermore, d_{eff} is defined so that it reproduces the usual definition of dimension for a simple QCD observable but it differs for composite observables.

Several examples may help illustrate d_{eff}. First consider some observable M that is a standard QCD quantity of mass dimension n. This quantity would satisfy $M(a, g) = a^{-n}\hat{M}(g)$, where $\hat{M}(g)$ is what is calculated on the lattice and the factor of a^{-n} is eventually put in by hand. Then for such an M we have

$$d_{\text{eff}}[M] = -\frac{a}{a^{-n}\hat{M}(g)} \frac{\partial}{\partial a} \left(a^{-n}\hat{M}(g)\right) = n .$$

Thus the dimension of quantities that we normally calculate is unaltered. However, for a composite object the answer can differ. For example,

$$d_{\text{eff}}\left[g_V^2 m_\mu^2/m_V^2\right] = d_{\text{eff}}\left[\hat{g}_V^2 a^2 m_\mu^2/\hat{m}_V^2\right] = -2$$

where $g_V^2 m_\mu^2/m_V^2$ is the leading piece of the vector-meson contribution to a_μ mentioned earlier. Thus d_{eff} captures the dimensionality of the QCD scales in this rather simple composite expression.

We can now apply the definition of d_{eff} to $a_\mu^{(2)}$ and we find

$$d_{\text{eff}}[a_\mu^{(2)}] = -2 \left(\int_0^\infty \frac{dQ^2}{Q^2} \omega(Q^2/m_\mu^2) Q^2 \frac{d\Pi_R}{dQ^2}\right) \left(\int_0^\infty \frac{dQ^2}{Q^2} \omega(Q^2/m_\mu^2)\Pi_R(Q^2)\right)^{-1} .$$

This quantity has a continuum limit. It is rather easy to show that $d_{\text{eff}}[a_\mu^{(2)}] < 0$, making it clear that $a_\mu^{(2)}$ acts like an observable with a negative mass dimension. Additionally, for $m_\mu \to 0$, we have $d_{\text{eff}} \to -2$, and for $m_\mu \to \infty$, we can show that $d_{\text{eff}} \to 0$. For an intermediate mass, this quantity must be calculated nonperturbatively. For the muon, we find

$$d_{\text{eff}}[a_\mu^{(2)}] = -1.887\,(5)$$

which clearly indicates that $a_\mu^{(2)}$ behaves much more like a mass dimension -2 quantity than a dimensionless observable.

2.3 Modified lattice method for $a_\mu^{(2)}$

Having diagnosed the difficulty in $a_\mu^{(2)}$, first with dimensional analysis and then a model argument, and having provided a clean definition of the problem using d_{eff}, we can now attempt to remedy it. In the end, we will define a modified quantity $a_{\overline{\mu}}^{(2)}$ that has the same physical limit as $a_\mu^{(2)}$ yet satisfies $d_{\text{eff}}[a_{\overline{\mu}}^{(2)}] = 0$. Since the physical values of both observables are the same, we can safely use either quantity to perform the computation. Furthermore, our observation that $d_{\text{eff}} = 0$ will provide a theoretical explanation for why $a_{\overline{\mu}}^{(2)}$ should lend itself to an easier calculation.

Starting with the observation that $d_{\text{eff}}[a_\mu^{(2)}] \neq 0$, we sought a minimal way to modify $a_\mu^{(2)}$ to eliminate this unexpected dependence on the lattice spacing. This is caused by the fact that m_μ is an external scale and not capable of absorbing the dependence on a. The solution we came upon was to insert the factor H_{phys}^2/H^2 as follows

$$a_{\overline{\mu}}^{(2)} = \alpha^2 \int_0^\infty \frac{dQ^2}{Q^2} \omega\left(\frac{Q^2}{H^2} \cdot \frac{H_{\text{phys}}^2}{m_\mu^2}\right) \Pi_R(Q^2) = \alpha^2 \int_0^\infty \frac{d\hat{Q}^2}{\hat{Q}^2} \omega\left(\frac{\hat{Q}^2}{\hat{H}^2} \cdot \frac{H_{\text{phys}}^2}{m_\mu^2}\right) \Pi_{\text{lat}}(\hat{Q}^2), \quad (2.5)$$

where H is some hadronic scale and H_{phys} is its physical limit value in physical units. Additionally, the value of H is understood as being calculated at the same m_{PS} as $a_{\overline{\mu}}^{(2)}$. Each choice of H gives rise to a distinct new observable $a_{\overline{\mu}}^{(2)}$. We will shortly pick a favored H, so the dependence on H in defining $a_{\overline{\mu}}^{(2)}$ is suppressed. By construction, this quantity has the same physical limit as the standard definition and eliminates the unwanted dependence on the lattice spacing,

$$\lim_{m_{PS} \to m_\pi} a_{\overline{\mu}}^{(2)} = a_\mu^{(2)} \qquad \text{and} \qquad d_{\text{eff}}[a_{\overline{\mu}}^{(2)}] = 0.$$

This modification completely eliminates the unwanted a dependence, but it does not automatically weaken the quark mass dependence. We know that the vector-mesons make a dominant contribution to $a_\mu^{(2)}$ of the form $g_V^2 m_\mu^2/m_V^2$ and that g_V, shown in figure 3, is only weakly m_{PS} dependent. This suggests choosing $H = m_V$. Other choices have been examined in [1] but we will use $H = m_V$ exclusively in these proceedings when discussing the modified approach.

The results for $a_{\overline{\mu}}^{(2)}$ are given in figure 4. As $a_{\overline{\mu}}^{(2)}$ is now a proper dimensionless observable composed of only QCD scales, it behaves like any other dimensionless quantity, as we can check by comparing with the g_V in figure 3. Additionally, the choice $H = m_V$ absorbs much of the m_{PS} dependence that has troubled previous calculations using the standard method. All indications are that the systematic errors are relatively mild. Additionally, we have checked that disconnected diagrams do not rise above the statistical errors shown in figure 4. The extrapolated value is given in table 2 and is consistent with the estimated $n_f = 2$ piece of the experimental determination. More importantly, it is encouraging that the resulting error on the physical limit value of $a_\mu^{(2)}$ is already within a factor of $3-4$ of the experimental determination using equation 2.3.

2.4 Comparison of current lattice calculations of $a_\mu^{(2)}$

Several groups have performed calculations of $a_\mu^{(2)}$ with both $n_f = 2$ [1, 10] and $n_f = 3$ [14, 9], and a first $n_f = 4$ calculation is underway [8]. To compare results, we focus on the standard method for this section. First, we can examine the lattice calculations for $n_f = 2$, which are shown in figure 5. There we find agreement between both computations, including their extrapolated values,
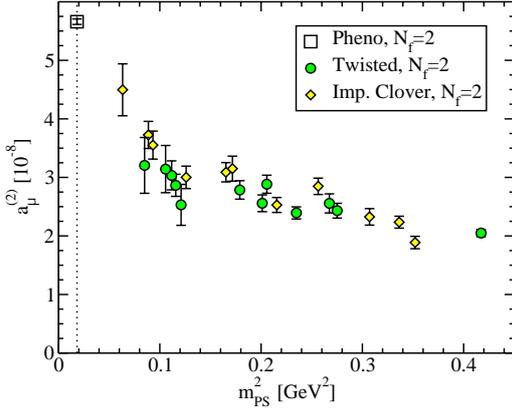
Figure 5: Two-flavor lattice calculations of $a_\mu^{(2)}$. The calculations are from [1] ("Twisted") and [10] ("Imp. Clover").
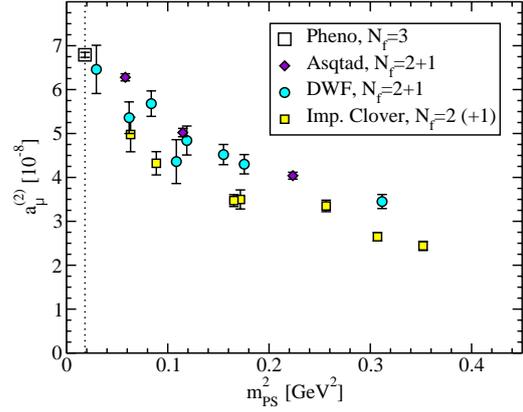
Figure 6: Three-flavor lattice calculations of $a_\mu^{(2)}$. The results are from [14] ("Asqtad"), [9] ("DWF") and [10] ("Imp. Clover").

which are given in table 2. These results were calculated using different actions, at least two lattice spacings, multiple physical volumes, a broad range of pion masses, and different treatments of the low Q^2 extrapolations of $\Pi(Q^2)$. The level of agreement is rather compelling for these two calculations. Additionally, it appears that the calculation of [10] shows a rapid rise as m_{PS} is lowered, which is consistent with the model-dependent expectations from the vector-meson contribution discussed previously.

We now turn our attention to the $n_f = 3$ calculations shown in figure 6. The situation here appears to be less compelling than for $n_f = 2$, but we must take some care before reaching such a conclusion. A detailed comparison requires a bit more space than allowed in these proceedings, so we will limit ourselves to commenting on one conceptual issue that is important to understand before making any definitive statements. When comparing the $n_f = 3$ results, we must consider how the strange quark mass is determined. Unless the chosen renormalization conditions match, there is no reason why these curves would generally agree. The only expectation is that the values extrapolated to $m_{PS} = m_\pi$ must agree when all other uncertainties have also been controlled for. This seems to be the case in figure 6. Additionally, the extrapolated values given in [9] and [10] (also given in table 2) do agree. (The work of [14] did not cite a final result but it overlaps with the calculation of [9] for all three values of m_{PS} used in [14].) Further understanding is needed for $n_f = 3$, but the results of the lattice calculations may be more encouraging than is reflected in a simple head-to-head comparison as done in figure 6.

3. Leading-order QCD correction to the electron magnetic moment

We now turn our discussion to a sequence of examples illustrating the application of the modified method of [1]. The first two examples are simple extensions to the other two leptons but nonetheless provide nontrivial tests of the new method. Besides, these are first lattice calculations of both quantities. In [1], the leading-order QCD contributions to the electron and tau magnetic moments were also calculated, $a_e^{(2)}$ and $a_\tau^{(2)}$. The electron magnetic moment is measured to a precision of 0.28 parts-per-trillion [15]. The lightness of the electron makes a_e significantly less dependent
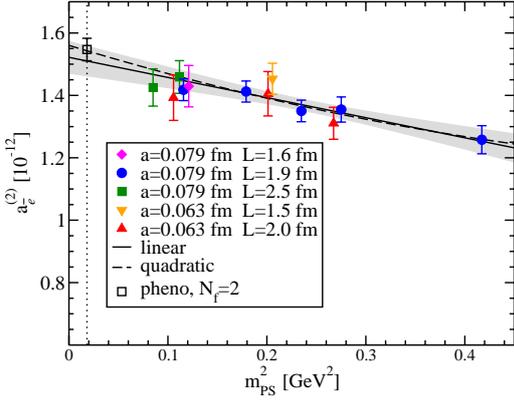
Figure 7: Modified method $a_{\bar{e}}^{(2)}$.
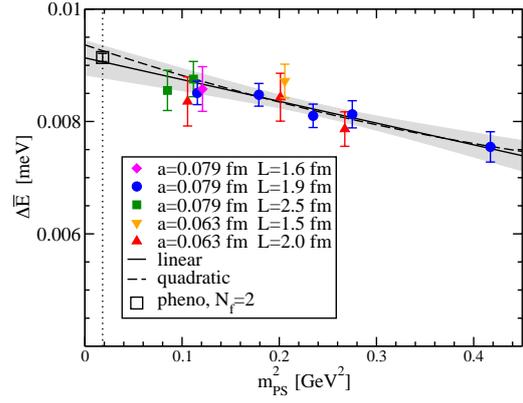
Figure 8: Modified method $\Delta \overline{E}$.

on QCD corrections but the enhanced precision of the experimental measurements overcomes the reduced sensitivity. The current measurement of a_e is so precise that it is in fact used to determine α. The standard model is then tested by comparing this value to other determinations of α. These comparisons have reached the precision that QCD effects of $a_e^{(2)}$ can not be ignored. However, the precision on a_e is not yet high enough to probe the error on $a_e^{(2)}$, so there is no pressing experimental need for higher precision $a_e^{(2)}$ determinations.

For our purposes, $a_e^{(2)}$ provides a test of the modified method that is sensitive to only the extreme lowest Q^2 scales. To a high accuracy, $a_e^{(2)}$ can be approximated as

$$a_e^{(2)} = \frac{4}{3}\alpha^2 m_e^2 \left. \frac{d\Pi_R(Q^2)}{dQ^2}\right|_{Q^2=0} + \mathcal{O}(m_e/\Lambda)^4.$$

This approximation is not used in [1], but we mention it in order to illustrate that $a_e^{(2)}$ probes essentially just the derivative of $\Pi(Q^2)$ at $Q^2 = 0$. It also illustrates in a simple way again the idea that $a_e^{(2)}$ may behave differently from a typical dimensionless observable. In the case of $a_e^{(2)}$, the approximation above strongly suggests that it will behave very much like a mass dimension -2 observable. This can be made precise by noting that

$$d_{\text{eff}}[a_e^{(2)}] = -1.999984\,(1).$$

The results for $a_e^{(2)}$ from [1] are shown in figure 7 using the modified method. The behavior of $a_e^{(2)}$ is very similar to $a_\mu^{(2)}$ and agrees with the estimated $n_f = 2$ piece of the experimental measurement.

Additionally, the leading QCD vacuum-polarization correction to the $2P-2S$ Lamb shift of muonic-hydrogen is also proportional to the slope of $\Pi(Q^2)$ at $Q^2 = 0$ and hence closely related to $a_e^{(2)}$. This correction is given in [16], with m_r the reduced mass of the $\mu-p$ system, as

$$\Delta E = 2\pi \alpha^5 m_r^3 \left. \frac{d\Pi_R}{dQ^2}\right|_{Q^2=0} \quad \text{and} \quad \Delta \overline{E} = 2\pi \alpha^5 m_r^3 \left. \frac{d\Pi_R(Q^2/H_{\text{phys}}^2 \cdot H^2)}{dQ^2}\right|_{Q^2=0}.$$

The second form is the modified approach for ΔE and results from a consistent treatment of external scales as discussed thoroughly in section 5. The results for $\Delta \overline{E}$ are shown in figure 8.
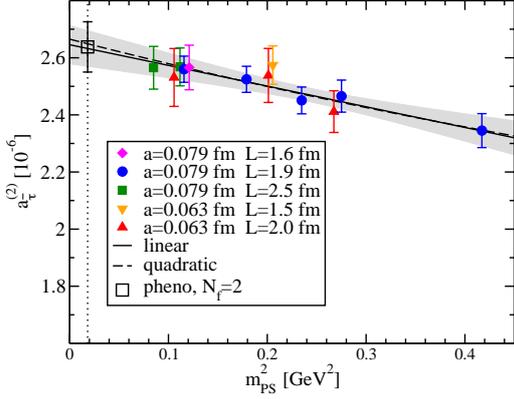
Figure 9: Modified method $a_{\overline{\tau}}^{(2)}$.
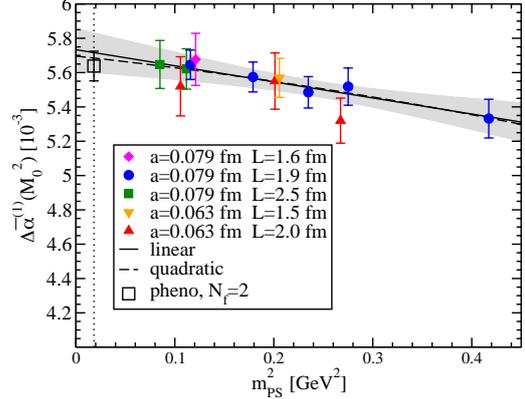
Figure 10: Modified method $\Delta\overline{\alpha}^{(1)}(M_0^2)$.

4. Leading-order QCD correction to the tau magnetic moment

The magnetic moment of the tau is substantially more sensitive to potential new physics than that of the muon, but it has not been experimentally measured. There are experimental bounds on a_τ [17], but more interesting to us is that $a_\tau^{(2)}$ can be determined by the same analysis used for $a_\mu^{(2)}$ and $a_e^{(2)}$. Additionally, due to the heaviness of the tau, it is sensitive to a different range of QCD scales. In fact,

$$d_{\text{eff}}[a_\tau^{(2)}] = -0.936\,(13)$$

indicates that it behaves quite a bit different than $a_\mu^{(2)}$ and $a_e^{(2)}$ and more like a mass dimension -1 observable. In fact, applying the standard method to $a_\tau^{(2)}$ leads to a reasonable calculation. However, the arguments for the modified method still apply here and it is yet another test of the approach. The results for $a_{\overline{\tau}}^{(2)}$ are shown in figure 9. Again, the resulting observable has a mild m_{PS} dependence. Furthermore, it agrees with the estimated $n_f = 2$ piece of the dispersive result, determined from equation 2.3, providing more confidence in both the modified method and the simple prescription for analyzing the n_f dependence of $R(s)$. As figure 9 shows, the lattice determination of $a_\tau^{(2)}$ is already more accurate than its experimental determination, suggesting that future measurements of a_τ can in fact rely on a fully nonperturbative determination of $a_\tau^{(2)}$ without sacrificing any precision once $n_f = 4$ lattice calculations have been completed.

5. Leading-order QCD contribution to the running of the QED coupling

In order to further demonstrate and understand the modified method of [1], we have applied the same idea to the determination of the leading-order QCD corrections to the running of α. This is the first lattice calculation of this quantity and all results discussed in these proceedings are preliminary. The running of α is normally treated by introducing an effective coupling given by summing all one-particle irreducible bubble insertions in the photon propagator. This results in

$$\alpha(Q^2) = \frac{\alpha}{1 - \Delta\alpha(Q^2)}.$$

The QCD contribution $\Delta\alpha^{\text{QCD}}$ is again expanded in α. The leading-order correction is

$$\Delta\alpha^{(1)}(Q^2) = 4\pi\alpha\,\Pi_R(Q^2)\,.$$

The value of $\alpha(Q^2 = 0)$ is just the usual coupling α, which is known to a relative precision of $1 \cdot 10^{-9}$. However, after evolving α to a high scale, say the Z-boson pole at $Q^2 = M_Z^2$, the relative precision on $\alpha(M_Z^2)$ drops to $1 \cdot 10^{-4}$ [6], making $\alpha(M_Z^2)$ one of the more poorly known fundamental parameters in high energy predictions. Similar to a_μ, the dominant uncertainty in this evolution is due to hadronic corrections, which is then passed into every high energy process through the use of the running coupling $\alpha(M_Z^2)$. This has larger impact than one might have naively expected. As one example, a recent global analysis by the Gfitter collaboration determined the Higgs mass to be $m_H = 44^{+62}_{-43}$ GeV, if the experimental determination of $\Delta\alpha(M_Z^2)$ was not included in the fit and found $m_H = 96^{+31}_{-24}$ GeV if it was [18].

The treatment of the external scales for $a_l^{(2)}$ introduced earlier uniquely fixes the treatment of the now external scale Q^2 in $\Delta\alpha(Q^2)$. To see this, we can simply rewrite equation 2.5 as

$$a_{\bar{l}}^{(2)} = \alpha^2 \int_0^\infty \frac{dQ^2}{Q^2}\,\omega\left(Q^2/m_l^2\right)\Pi_R\left(Q^2/H_{\text{phys}}^2 \cdot H^2\right)\,.$$

This suggests rather clearly that we should consider the following modified definition of $\Delta\alpha^{(1)}$

$$\Delta\overline{\alpha}^{(1)}(Q^2) \equiv 4\pi\alpha\,\Pi_R(Q^2/H_{\text{phys}}^2 \cdot H^2)\,.$$

Just as for $a_{\bar{l}}^{(2)}$, this new quantity explicitly has the correct physical limit but also satisfies $d_{\text{eff}} = 0$.

We can examine the consequences of this definition by first focusing on $Q^2 = M_0^2$ with $M_0 = 2.5$ GeV, which is a common matching scale for phenomenological work. The lattice calculation is shown in figure 10. We see that, just as for each of the $a_l^{(2)}$ calculations, the modified definition results in a rather mild looking extrapolation to the physical point, giving $\Delta\alpha^{(1)}(M_0^2) = 5.72\,(12) \cdot 10^{-3}$. We can also apply the same treatment of the n_f dependence of the experimentally determined $R(s)$ to $\Delta\alpha^{(1)}$ resulting in $\Delta\alpha^{(1)}(M_0^2) = 5.60\,(06) \cdot 10^{-3}$. The preliminary lattice computation results in an uncertainty that is now only twice the error of the experimentally determined quantity, suggesting that lattice calculations could be a competitive, if not superior, way to determine $\Delta\alpha(Q^2)$ at least for low scales.

Now, we can repeat the analysis for all Q^2 and determine the QCD induced running of $\alpha(Q^2)$. This is shown in figure 11. By comparing results with different lattice spacings, we notice significant lattice artifacts only for $Q^2 \gtrsim 7$ GeV^2. This appears to be just a mild obstacle to an accurate determination of $\Delta\alpha(Q^2)$ in the relevant low Q^2 regime. The scale of $Q^2 = M_0^2$ was chosen because perturbation theory becomes reliable for yet larger Q^2. To run α to higher scales, we have determined α_s by matching $\Pi(Q^2)$ to the perturbative expectations for the Q^2 regions that can be reached in lattice calculations and then determined $\Delta\alpha^{(1)}(Q^2)$ at larger scales through

$$\Delta\alpha^{(1)}(M_Z^2) = \Delta\alpha^{(1)}(M_0^2) + (\Delta\alpha^{(1)}(M_Z^2) - \Delta\alpha^{(1)}(M_0^2))\,,$$

where the perturbative expression for $\Delta\alpha^{(1)}(M_Z^2) - \Delta\alpha^{(1)}(M_0^2)$ is available at 5 loops [19].
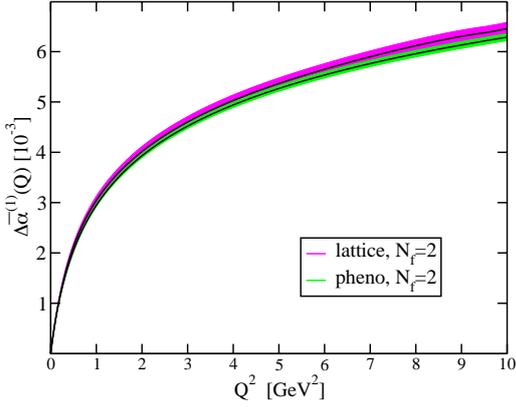
Figure 11: Modified method $\Delta\overline{\alpha}^{(1)}(Q^2)$.
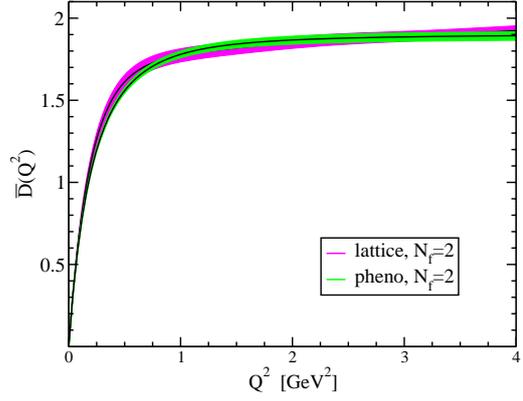
Figure 12: Modified method $\overline{D}(Q^2)$.

We note that to determine α_s, it appears to be better to calculate the Adler function $D(Q^2) = d\Pi(Q^2)/d\ln(Q^2)$. To consistently apply our treatment of the external scale Q, we define a modified Adler function

$$\overline{D}(Q^2) = D(Q^2/H_{\text{phys}}^2 \cdot H^2).$$

The results of a preliminary calculation with the modified technique are shown in figure 12.

6. Next-to-leading-order QCD contribution to the muon magnetic moment

The precision of the current BNL measurement of a_μ already requires that the next-to-leading-order QCD correction $a_\mu^{(3)}$ be accounted for. Most of the diagrams involve insertions of the vacuum-polarization correction into lower order QED diagrams, but a new QCD contribution, called light-by-light, also occurs at this order.

6.1 Vacuum-polarization corrections

The vacuum-polarization correction can be inserted once or twice into any photon line of a two-loop or one-loop QED diagram, respectively. This results in 16 diagrams that involve one oc-currence of $\Pi(Q^2)$ and one diagram with two insertions of $\Pi(Q^2)$. Example diagrams are shown in figure 13. Expressions in various forms are available for these corrections when expressed as integrals over R. The analytic continuation to Euclidean space is complicated for some of these contributions, but it appears that all vacuum-polarization contributions to $a_\mu^{(3)}$ can be calculated in Euclidean space. A preliminary calculation using the modified approach[1], shown in figure 14, gives $a_\mu^{(3,\text{vp})} = -7.99\,(20) \cdot 10^{-10}$. The uncertainty includes only statistical errors but the systematic un-certainties appear to be small. For comparison, the $n_f = 2$ piece of the experimental measurement is $a_\mu^{(3,\text{vp})} = -7.94\,(16) \cdot 10^{-10}$. Further study is underway, but the initial results for the vacuum-polarization contribution to $a_\mu^{(3)}$ seem to agree with the expectations from the experimental mea-surements and have a nearly comparable uncertainty. Most importantly, the precision of the lattice result is better than the accuracy expected for the future muon g-2 measurements, so it seems that

---

[1] At the conference, only a partial accounting of the diagrams was given and resulted in a different value. The result reported here accounts for all vacuum-polarization contributions to $a_\mu^{(3)}$.
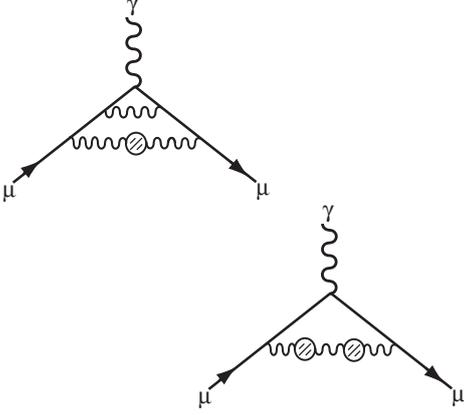
Figure 13: Example diagrams for $a_\mu^{(3,\mathrm{vp})}$.
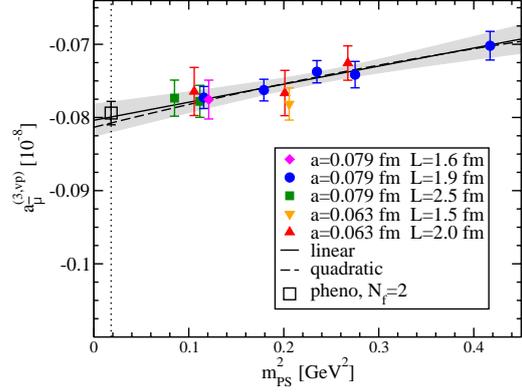
Figure 14: Modified method $a_{\overline{\mu}}^{(3,\mathrm{vp})}$.

lattice QCD should be quite capable of determining the higher-order vacuum-polarization contributions at the required precision.

6.2 Light-by-light corrections

In contrast to the vacuum-polarization corrections, the light-by-light contributions to $a_\mu^{(3)}$ represent a real challenge. There are ongoing lattice studies by several groups [20, 21, 22], each using different methods but still all exploratory. The uncertainty on the light-by-light correction $a_\mu^{(3,\mathrm{lbl})}$ is nearly as large as that of $a_\mu^{(2)}$ and there are open questions regarding the methods currently used for its determination, so a nonperturbative calculation of $a_\mu^{(3,\mathrm{lbl})}$ is highly desirable. However, a lattice calculation of one piece of the higher-order contribution is less satisfying than a complete lattice calculation of both the leading-order and next-to-leading-order corrections. It now appears that the vacuum-polarization pieces should be calculable, so the light-by-light contribution is the only remaining piece needed for a completely nonperturbative determination of a_μ^{QCD} accurate to $\mathscr{O}(\alpha^3)$. We can only hope that this will encourage an even greater effort within the lattice community to tackle the desperately needed light-by-light contribution.

7. Conclusions

We have discussed several examples of important measurements that receive sizable hadronic corrections. The muon g-2, which hints at beyond-the-standard-model physics, is the most pressing observable, but $\Delta\alpha(Q^2)$ may in fact have a much broader impact on precision standard model predictions. Using a modified lattice approach, the leading QCD corrections to both of these observables appear to be reliably calculable. To further explore the new method, we have also examined the leading corrections to the electron and tau leptons and the Lamb shift in muonic-hydrogen. We have calculated the Adler function, which can be matched to perturbation theory to determine the strong coupling. Lastly, we have worked out methods to examine all the vacuum-polarization corrections at the next-to-leading order. In several cases, the currently reached precisions on these quantities are approaching that of the corresponding experimental determinations. This indicates that fully nonperturbative determinations of QCD corrections to electroweak observables may be

feasible at the precisions needed by future experimental measurements that aim to discover or constrain physics beyond the standard model.

8. Acknowledgments

References

[1] X. Feng, K. Jansen, M. Petschlies, and D. B. Renner, Phys.Rev.Lett. **107**, 081802 (2011), arXiv:1103.4818.

[2] Muon $g - 2$ Collaboration, G. Bennett *et al.*, Phys.Rev.Lett. **92**, 161802 (2004), hep-ex/0401008.

[3] F. Jegerlehner and A. Nyffeler, Phys.Rept. **477**, 1 (2009), arXiv:0902.3360.

[4] B. L. Roberts, Chin.Phys. **C34**, 741 (2010), arXiv:1001.2898.

[5] A. Toyoda *et al.*, Proceedings of NUFACT 11 (2011), arXiv:1110.1125.

[6] M. Davier, A. Hoecker, B. Malaescu, and Z. Zhang, Eur.Phys.J. **C71**, 1515 (2011), arXiv:1010.4180.

[7] http://www-com.physik.hu-berlin.de/~fjeger/software.html.

[8] X. Feng, G. Hotzel, K. Jansen, M. Petschlies, and D. B. Renner, in preparation (2012).

[9] P. Boyle, L. Del Debbio, E. Kerrane, and J. Zanotti, Phys.Rev. **D85**, 074504 (2012), arXiv:1107.1497.

[10] M. Della Morte, B. Jäger, A. Jüttner, and H. Wittig, JHEP **1203**, 055 (2012), arXiv:1112.2894.

[11] Private communication from F. Jegerlehner.

[12] Private communication from M. Davier, A. Hoecker, B. Malaescu and Z. Zhang.

[13] T. Blum, Phys.Rev.Lett. **91**, 052001 (2003), hep-lat/0212018.

[14] C. Aubin and T. Blum, Phys.Rev. **D75**, 114502 (2007), hep-lat/0608011.

[15] D. Hanneke, S. Fogwell, and G. Gabrielse, Phys.Rev.Lett. **100**, 120801 (2008), arXiv:0801.1134.

[16] R. Faustov and A. Martynenko, Eur.Phys.J.direct **C1**, 6 (1999), hep-ph/9906315.

[17] Particle Data Group, K. Nakamura *et al.*, J.Phys.G **G37**, 075021 (2010).

[18] Gfitter Group, M. Baak *et al.*, (2011), arXiv:1107.0975.

[19] P. Baikov, K. Chetyrkin, and J. H. Kuhn, Phys.Rev.Lett. **101**, 012002 (2008), arXiv:0801.1821.

[20] M. Hayakawa, T. Blum, T. Izubuchi, and N. Yamada, PoS **LAT2005**, 353 (2006), hep-lat/0509016.

[21] QCDSF Collaboration, P. Rakow *et al.*, Talk at Lattice 2008 by P. Rakow.

[22] JLQCD Collaboration, E. Shintain *et al.*, PoS **LAT2009**, 246 (2009), arXiv:0912.0253.